DOI: *10.1007/s12583-017-0940-4*

Origin and geodynamic implications of concealed granite in Shadong tungsten deposit, Xinjiang China: zircon U-Pb chronology, geochemistry, and Sr-Nd-Hf isotopeconstraint[1]

Chao Chen[1], Xinbiao Lü[1,2*],ChunMing Wu[1], Xiao Jiang[3], Chen Mao[2]

1.*Institute of Geological Survey, China University of Geosciences, Wuhan 430074, China*

2. *Faculty of Earth Resources, China University of Geosciences, Wuhan430074, China,*

3.*No.6 Geological Survey Team,Bureau of Xinjiang GeologicalExploration, Hami839000, China,*

Abstract: Shadong deposit is the first large-scaletungsten deposit found in East Tianshan Orogenic Belt, and the geologic characteristics of the deposit indicate that the deeply concealed granite bodyis genetically related with the mineralization. LA-ICPMS U-Pb age of zircons from the Shadong concealed granite obtained in this research is 239±2.0Ma, belonging to Middle Triassic. The whole rock samples are metaluminousto slightly peraluminous (A/CNK=0.95–1.02) with low contents of SiO_2(64.0–68.5wt.%) and low K_2O/Na_2O ratios(0.73–0.96). The samples reveal enrichmentof K, Rb, Th and depletion of Nb, Ta, P ,Ti and have a negative slope from La to Lu (La_N/Yb_N=16.29–36.8)with weak negative Eu anomaly(Eu/Eu*= 0.71–0.82).Initial $^{87}Sr/^{86}Sr$ ratios of whole rock range from 0.70659–0.70775, εNd(t)values range from -1.77 to -2.53 and εHf(t)values of zircon are between 2.54 and 4.90. The lithogeochemistry and Sr-Nd-Hf isotopiccharacteristics revealed that the concealed granite in Shadong tungsten deposit belong to I-type granite, and occurred in anintraplate tectonic setting. The magma mixing during intraplating of mantle derived magma intruding into the crustin Indosinian periodis the major formation mechanism of the granite.Of which, the proportion of mantle derived magma range from58% to 60%, and thecrustalmaterials are mainly the metamorphic basement of Xingxingxia Group of MesoproterozoicChangcheng system, which may provide the main source of ore forming metals of Shadong tungsten deposit.

Key words: East Tianshan, Shadong tungsten deposit, Crust-mantle interaction, Zircon U-Pb chronology, lithogeochemistry, Sr-Nd-Hf isotope

[1]Corresponding author:Xinbiao Lü; Email: 748555304@qq.com

This study was financially supported by the project of Metallogical condition research and ore prospecting target area evaluation of copper-gold-iron metallogenic belt in Kuruktag (2011BAB06B04).

0 INTRODUCTION

Central Asian orogenic belt(CAOB) is a giant orogenic belt which was formed by the continuous subduction of the Paleo-Asian Ocean underneath the Siberian plate, Sino Korean plate and Tarim plate in the Neoproterozoic-Paleozoic Era (Kröner et al., 2008; Xiao et al., 2013, 2014)(Fig. 1a). East Tianshan Orogenic Belt in Xinjiang is an important part of Central Asian orogenic belt, which is divided into three tectonic units: from north to south,Dananhu-Tousuquan Volcanic Arc, Jueluotag Are-Basin system and Central Tianshan massif (Dong et al., 2011; Deng et al., 2017) (Fig. 1b).The bilateral subduction of the Junggar Ocean and Southern Tianshan Ocean to the Central Tianshan massif resulted in the large-scale Paleozoic magmatism and mineralization (Yang et al., 2012; Li et al., 2013; Tang et al., 2013).In recent years, it has been gradually realized that the magmatism of East Tianshan in Indosinian Period was also highly developed, and a large number of granites with positive εNd(t) values and young Nd model ageswere found, indicating mantle underplating in this region (Hong et al., 2004; Zhang, 2005a; Gu et al., 2006; Wang et al., 2008). It is regarded that the origin of a series of tungstenand molybdenum deposits in this period aregenetically related to the above granites(Jiang et al., 2006;Zhu et al., 2013; Wu et al., 2013; Wang et al., 2016; Wu et al., 2017). Compared to molybdenum deposit, the research degree of tungsten deposit in this region is still at a low level. Shadong tungsten deposit is the fisrt large-scale tungsten deposit found in East Tianshan area.Field investigation indicates that the mineralizetion is closely related to the concealed granite intrusionin the ore district (Tang, 2015). However, the age and origin of the ore-forminggranite still remain unclear and geodynamicsetting is not confirmed, which restrict the understanding of ore genesis of Shadong deposit.

In this contribution, we report new data for the ore-forming graniticrocks, including zircon U–Pb isotope ages, major and trace element concentrations and Sr–Nd-Hf isotope compositions;and thereby, comprehensively define the ages and geneses ofthe granitic rocks and discuss its origin and geodynamic-metallogenic implications.

1REGIONAL GEOLOGY

The research area is located in the south central part of the Central Tianshan massif and at the northeastern margin of the Tarim Basin(Fig. 1b, 1c).The strata in a chronological order include: (1)Xingxingxia Group of MesoproterozoicChangcheng system (Chx), the main lithologyare mica-quartzose schist, biotiteplagiogneiss, and plagioclase-hornblende schist, etc. (2) Kawabulake Group of MesoproterozoicJixian System (Jxkw), the main lithologyare biotiteplagiogneiss, biotiteplagioclasegranulite, and marble, etc. (3) Cambrian Xidashan Group, the main lithologyare siliceous rock and shale, etc(Xiao et al., 2008, 2013). Main structures in this region include NE-NNE trending faults, which are, from north to south, Alatag fault, Alatag-Jianshanzi fault, and Kalatage-Shiyingtan fault successively. Of which, Alatag-Jianshanzi fault passes through the Shadong tungsten deposit, and controls the distribution of ore body of the deposit together with its secondary faults. The intrusive rocksin this region are mainly Variscangranite, followed by granodiorite, diorite, mafic dikes, etc. Early Variscian intrusive rocks were distributed betweenAketage-Jianshanzi fault and Alatag deep fault, showing batholith shape, and the main lithologicfeatures are plagiogranite,granodiorite,fine-graindiorite, etc. Middle Variscian intrusive rocks are distributed around the intrusive rock of Early Variscian, which were produced showing in stock, dyke and dendritic shape, with themain lithologicfeatures of flesh red, grey white biotite granite. The rocks have undergone different degrees of brittle and ductile deformation, thus forming gneissic structure, and ductile deformation overlaying can be seen in the later period(Tang, 2015).

Intrusive rocks are distributed in the southeast part of the mine, the main lithologic features are Middle VariscanK-feldspar granite, biotite granite, and diorite, etc. Field inspection did not found anyhydrothermal alteration or tungsten mineralization in the surface intrusiverocks and the wall rocknear

the contact zone, showing the tungsten mineralization is notgenetically related to thesurface intrusiverocks in the ore district.

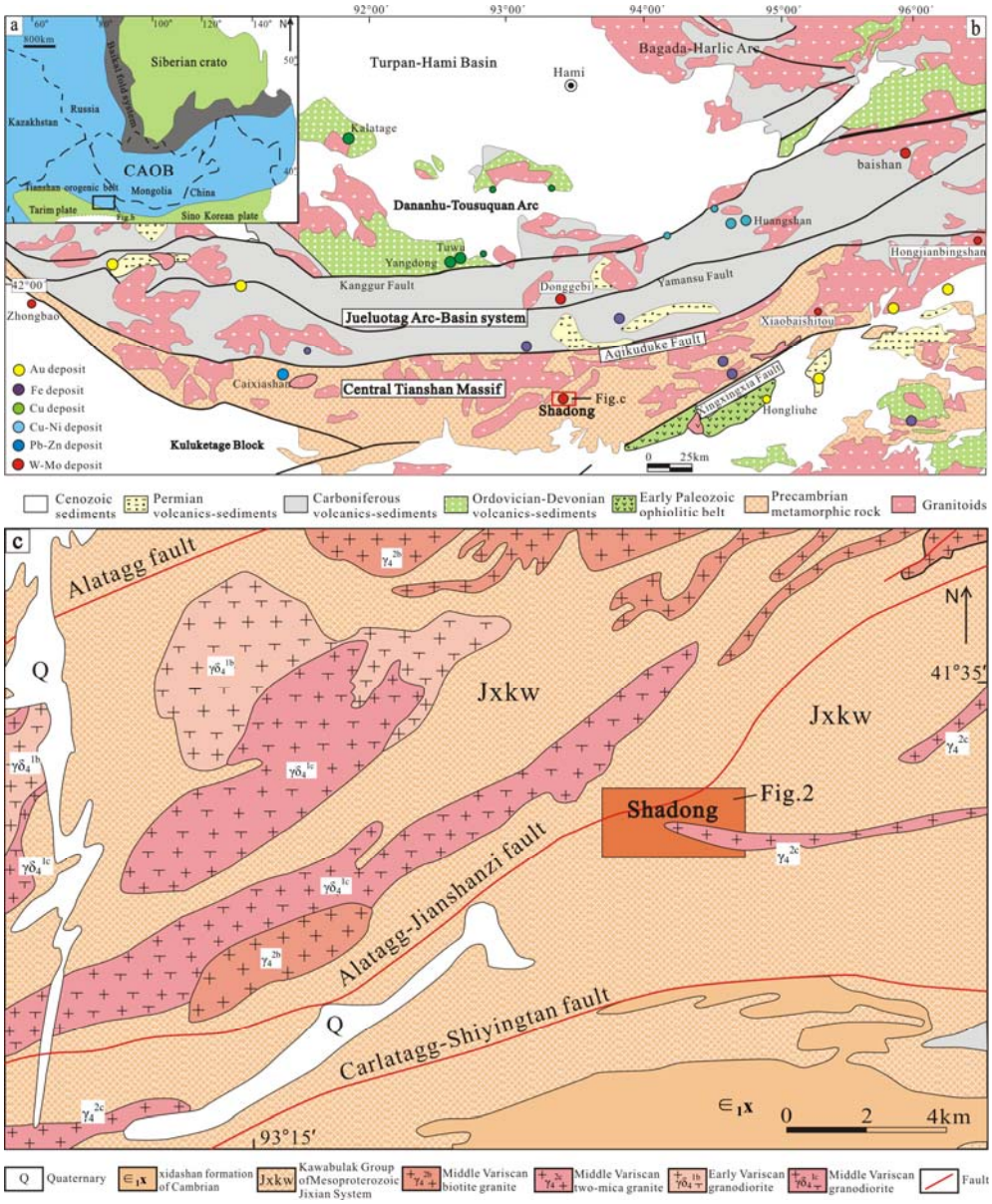

Figure1. (a) Sketch of CAOB tectonics (modified after Sengor and Natal'in, 1996); (b) Geology sketch map of Eastern Tianshan (modified after Deng *et al*., 2017). (c) Geology sketch map of peripheral rigion of Shadong ore district(modified after Jiang *et al*., 2012)

2DEPOSIT GEOLOGY

The stratain Shadong tungsten deposit mainly include the Kawabulak Group of MesoproterozoicJixian System and Tianhu Group of Qingbaikou System. Kawabulak Group is the main ore-bearing stratum, which can be divided into three sections from south to north according to the lithological differences: the lower section is mainly biotite plagiogneiss;the middle section is mainly dolomitic marble and marble; and the upper section is mainly biotite-plagioclasegranulite(Fig. 2).The strata show a NE-near EW trend , with an inclination of 345°–10° and a dip angle of 65–85°.

The main faults in the mining area are Alatag-Jianshanzi fault (F6) and its secondary faults (F1, F2, F3, F4, and F5). They are mainly reverse faults and transcurrent faults, and can be divided into three groups by trends: ①NEE trend (F5), ②NE-SW trend (F1, F2, and F4), ③NW-SE, (F3). Folds are

distributed in the central north part of the mine generally along NE~SW trend, and are spatially related to the distribution of ore body (Jiang et al., 2012; Tang, 2015).

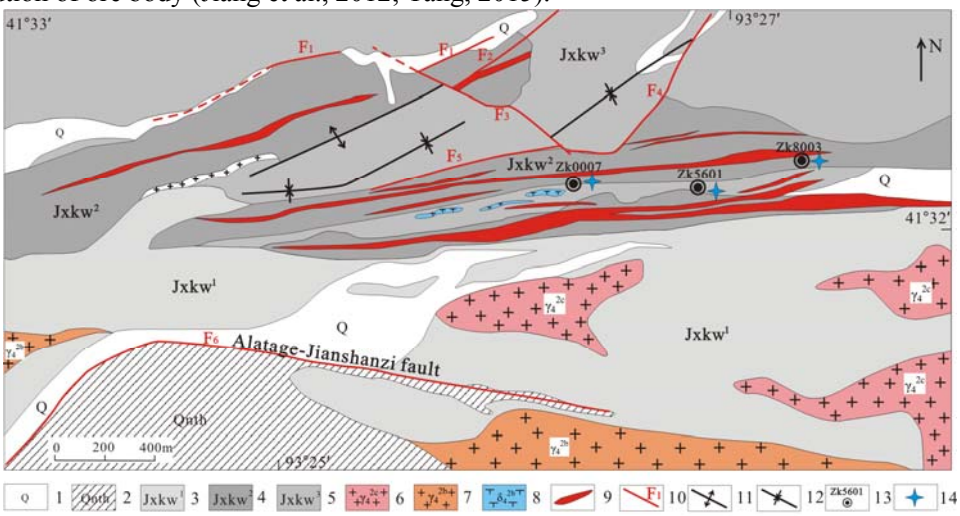

Figure 2. Geology map of Shadong ore district (modified from Jiang *et al*., 2012)

1. Quaternary system; 2. Tianhu Group of Qingbaikou System; 3. Gneiss of Kawabulak Group of Jixian System; 4. Marble of Kawabulak Group of Jixian System; 5. Leptynite of Kawabulak Group of Jixian System; 6. Two-mica granite in middle Variscan period; 7. Two-mica granite and biotite granite in middle Variscan period; 8. Diorite dike; 9. Tungsten ore body; 10. Fault; 11. Anticline; 12. Syncline; 13. Drill hole and number ; 14. Sampling location

Drilling showed that concealed granitic body exists deep in the mine, and the tungsten ore mainly occurs in the quartz vein filled in the fractures of the host rock (marble and biotiteplagiogneiss) (Fig. 3a, 3b, 3g) and the concealed granite (Fig. 3h), and partially occurs in the skarnizedcontact zone(Fig. 3c). The morphology of ore body mainly shows vein-like or stratiform-likeoccurrence (Fig.3d, 3e) due to the influence of structural fracture and interlayer fracture zone, followed by metasomatism disseminated mineralization(Fig. 3f).The general tendency of ore body is 325°–345°, the dip angle is 55°–65°, the strike length is 100m–5000m, the deepening length in deep part is 100~1000m, the average thicknessof ore body is 0.8–4.35m, and the average grade of WO_3 is 0.265%. Based on the lithology of the ore-bearinghost rock, the ore can be divided into marble type, gneiss type and skarn type; the main ore mineral is scheelite, and the gangue mineral combinations are calcite+dolomite+quartz+sericite+fluorite, feldspar+quartz+ biotite, diopside+tremolite+epidote+garnetsuccessively. The hydrothermalalteration mainlyincludes silicification, pyritization, sericitization, and greisenization, etc.According to the geological characteristics of the deposit, the genetic type of ore is preliminary considered as magmatic hydrothermal type and skarn type .

3SAMPLES DESCRIPTIONS AND ANALYTICAL METHODS

3.1 Description of samples

The granite body is located below 500 meters at depth with nearly EW trending, the main lithology of which is biotite monzonitic granite, and wall rocks are mainly marble of Kawabulak Group of Jixian System . In consideration of the influence of alteration on the contents of main elements of whole rock, the samples were all taken from the fresh and unalteredgranite core. Studied samples show a coarse grained texture and massive structure(Fig. 3h). These rocks are composed of the minerals such as quartz (25%–30%), plagioclase (30%–35%), microcline (20%–30%), biotite (7%–10%) and hornblende(2%–3%) (Fig. 3i), as well as the secondary minerals such as zircon, pyrite and sphene. In this research, eight granite samples were taken at 660-1040 meters deep (ZK0007, ZK5601 and ZK8003 drill holes). Detailed sampling locations are shown in Figure 2 and Table 2.

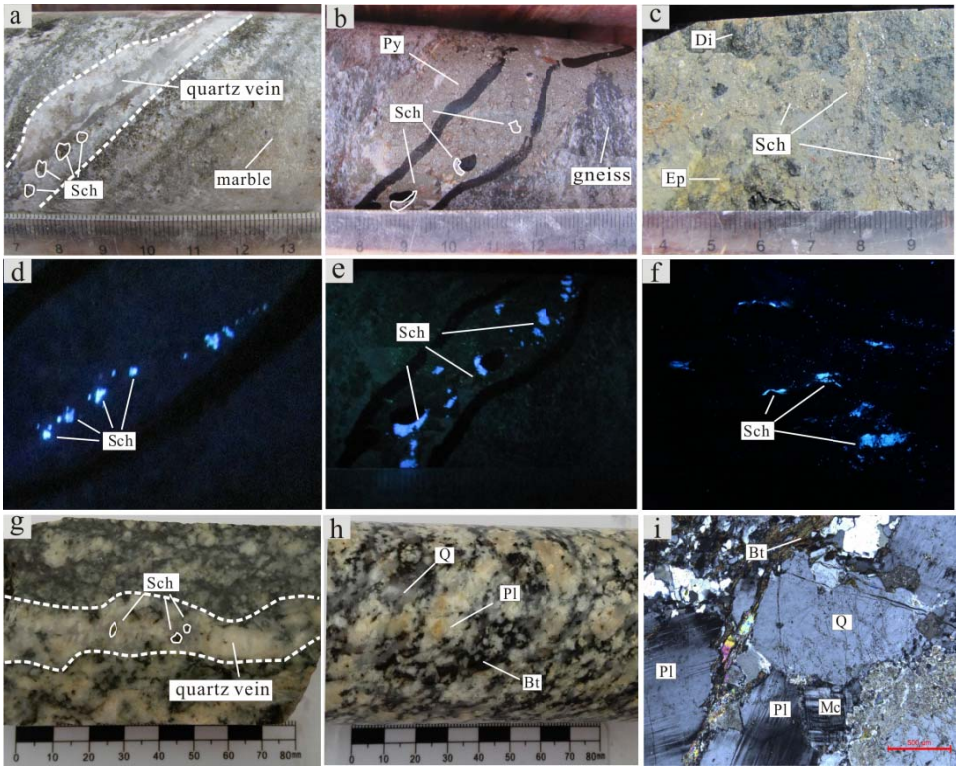

Figure3. Characteristic of scheelite ore and wall rock in Shadong ore district

a) Quartz vein with scheelite in marble wall rock; b) Scheelite with pyrite in gneiss wall rock;c) Diopside-epidote skarn scheelite ore; d) Figure 3a under the fluoresent light, vein-like scheelite;e) Figure 3b under the fluoresent light, vein-like scheelite; f) Figure 3c under the fluoresent light, disseminated scheelite;g) Quartz vein with scheelite in concealed granite core; h) Drilled core sample of biotite adamellite;i)Petrographic image of biotite adamellite;

Sch–scheelite, Py–pyrite, Di–diopside, Ep–epidote, Q–quartz, Pl–plagioclase, Mc–Microcline, Bt–biotite

3.2 Zircon LA-ICP-MS U-Pb Dating

Zircons were separated from one sample of thegranites (SD33) and documented with transmitted and reflectedlight as well as cathodoluminescence imagery to reveal their external and internal structures atthe State Key Laboratory of Geological Processes and MineralResources, China University of Geosciences in Wuhan,China. Laser ablation techniques were used for zircon agedeterminations.The analyses were completed withan Agilent 7500a ICP-MS, equipped with 193 nm excimerlasers. Zircon 91500 was used as agestandard (1062 Ma, Wiedenbeck et al., 1995) and NIST 610was used to optimize the trace element results. Spot diameterwas 32 μm. Analytical methodology is described indetail in Liu et al. (2008, 2010). The ageswere calculated using ICPMSDataCal software (ver 9.0,China University of Geosciences) (Liu et al., 2008) andConcordia diagrams were made by Isoplot/Ex ver3.7 (Ludwig,2003). Trace element compositions of zircon were calibratedagainst GSE-1G combined with internal standardization[29]Si (Liu et al., 2010). Errors on individual analyses by LAICP-MS are quoted at 95% (1 σ) confidence level.

3.3 Major and Trace Elements Analyses

Major elements were analyzed with a PAN analyticalAxios X-ray fluorescence spectrometer (XRF) at ALS Chemex(Guangzhou) Co Ltd. A calcined or ignited sample(0.9 g) is added to 9.0 g of Lithium Borate Flux (50%–50%$Li_2B_4O_7$–$LiBO_2$), mixed well and fused in an auto fluxerbetween 1050–1100°C. A flat molten glass disc is preparedfrom the resulting melt. This disc is then analyzed by X-rayfluorescence spectrometry. The precision of the XRF analysesat ALS Chemex is better than 5%.Trace element concentrations were determined with anElan 9000 at the same lab. A prepared sample (0.2g) isadded to lithium metaborate flux (0.9g), mixed well andfused in a furnace at 1000 °C. The resulting melt is thencooled and dissolved in 100 ml of 4% HNO_3/2% HClsolution. This solution is then analyzed by

inductively coupledplasma-mass spectrometry (ICP-MS). The precisionof the ICP-MS analyses at ALS Chemex is better than 10%for all elements.

3.4 Sr-Nd isotopes

Sr-Nd isotope analyses on X whole rock sampleswere carried out atGuangzhou Institute of Geochemistry, Chinese Academy of Sciences.Rb-Sr and Sm-Nd isotopes were determined using MC-ICP-MS . The detailed operation process can be seen from Zhang et al., (2002). The blanks were ~10 pg for Sm and Nd, and ~20 pg for Rb and Sr. $^{86}Sr/^{88}Sr$= 0.1194 and $^{146}Nd/^{144}Nd$=0.7219 were used for fractionation correction of Sr and Nd isotopes. The measured values for the LaJolla Nd standard and the SRM987 Sr standard were $^{143}Nd/^{144}Nd$= 0.511861±10 and $^{87}Sr/^{86}Sr$= 0.710263 ±10 during the period of data acquisition.

3.5 Zircon Hf isotopes

The zircon in-situ Hf isotope analyseswerecarried outin State Key Laboratory of Geological Processes & Mineral Resources of university (Wuhan), using a Neptune multiple- collector inductively coupled plasma mass spectrometry (LA-ICPMS) with 193nm laser sampling system. During analyzing, a beam spot diameter of 44μm, a laser impulse frequency of 10 Hz and a beam pulse energy of 100mJ were adopted. The detailed instrument operation conditions and experimental process can be seen fromHu et al., (2012). During the analyses, the $^{176}Hf/^{177}Hf$ ratios of the standard zircon (GJ-1) were 0.282013±0.000022 (2σ), agreeing with the recommended values (Li et al., 2010) within 2σ error.

4RESULTS

4.1 Zircon LA-ICP-MS U-Pb Dating

Zircon in granite are elongated, slabbyand transparent. The inherited zircon can be seen in some core parts. In cathodoluminescence images, zircon shows oscillatory zonations of typical magmatic origin (Fig. 4). The analyzed age data are listed in Table 1. Th/U ratios of zircon are between 0.47 and 0.73. REE contents of zircon are basically consistent, HREE contents are high with positive Ce anomaly and negative Eu anomaly. The above characteristics indicate that all zircon are ofmagmatic origin(Rowley et al., 1997; Hidaka et al., 2002; Whitehouse, 2003). $^{206}Pb/^{238}U$ ages of thirty points are in the range of 230±3.0Ma – 254±4.3Ma. The concordia age of 239±1.4Ma (MSWD=0.066) (Fig. 5a) and weighted average age of 239±2.0Ma (MSWD=2.9) (Fig. 5b) are obtained. Combined with the shape of zircon and the rare earth elements, we suggest that the zircon age analyzed can represent the magmatic intrusion age, which is identified as Early-Middle Triassic.

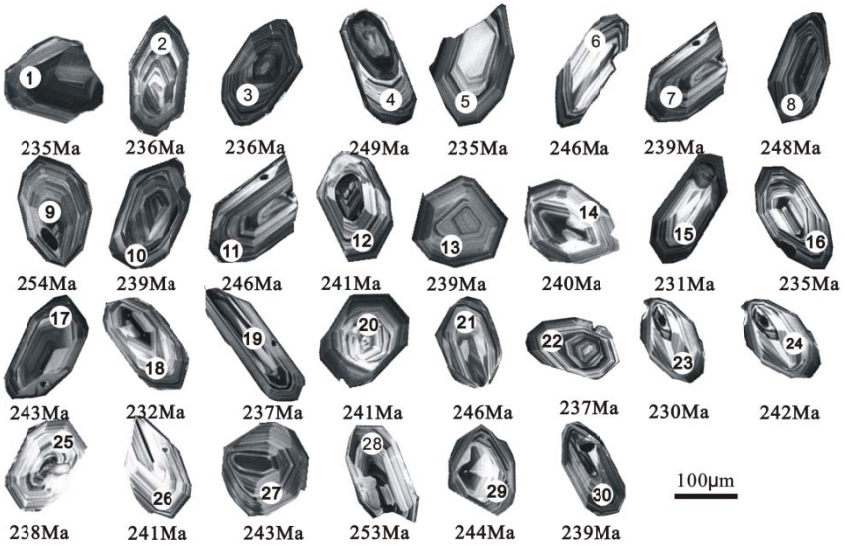

Figure 4. Cathodoluminescence(CL) image of shadong granite zircon

Table 1 Zircon U-Pb isotopic data of Shadong granite samples

Sample number	Th	U	Th/U	$^{207}Pb/^{206}Pb$		$^{207}Pb/^{235}U$		$^{206}Pb/^{238}U$		rho	$^{207}Pb/^{235}U$		$^{206}Pb/^{238}U$		$^{208}Pb/^{232}Th$	
	ppm	ppm		Ratio	1σ	Ratio	1σ	Ratio	1σ		Age (Ma)	1σ	Age (Ma)	1σ	Age (Ma)	1σ
SD33-1	748	1579	0.47	0.0510	0.0020	0.2603	0.0100	0.0372	0.0005	0.3287	235	8.1	235	2.9	251	6.5
SD33-2	581	1129	0.51	0.0516	0.0030	0.2618	0.0142	0.0373	0.0005	0.2613	236	11.5	236	3.3	242	8.3
SD33-3	517	928	0.56	0.0507	0.0026	0.2607	0.0129	0.0373	0.0005	0.2577	235	10.4	236	3.0	243	7.6
SD33-4	267	514	0.52	0.0511	0.0032	0.2754	0.0180	0.0394	0.0007	0.2784	247	14.4	249	4.5	255	10.2
SD33-5	277	525	0.53	0.0512	0.0038	0.2617	0.0193	0.0371	0.0006	0.2017	236	15.5	235	3.4	211	10.3
SD33-6	458	628	0.73	0.0514	0.0035	0.2744	0.0191	0.0389	0.0005	0.1921	246	15.2	246	3.2	239	8.0
SD33-7	410	775	0.53	0.0508	0.0030	0.2625	0.0150	0.0377	0.0005	0.2329	237	12.1	239	3.1	233	8.9
SD33-8	351	664	0.53	0.0512	0.0035	0.2722	0.0181	0.0392	0.0006	0.2162	244	14.4	248	3.5	237	9.2
SD33-9	258	471	0.55	0.0514	0.0032	0.2822	0.0174	0.0401	0.0007	0.2776	252	13.8	254	4.3	241	10.4
SD33-10	810	1261	0.64	0.0503	0.0025	0.2639	0.0134	0.0378	0.0004	0.2268	238	10.7	239	2.7	248	7.6
SD33-11	436	789	0.55	0.0518	0.0032	0.2723	0.0161	0.0389	0.0006	0.2588	245	12.8	246	3.7	247	8.5
SD33-12	577	841	0.69	0.0513	0.0027	0.2661	0.0137	0.0380	0.0006	0.3184	240	11.0	241	3.9	234	8.4
SD33-13	464	814	0.57	0.0509	0.0026	0.2649	0.0135	0.0377	0.0005	0.2542	239	10.9	239	3.0	234	8.7
SD33-14	887	1412	0.63	0.0510	0.0025	0.2642	0.0120	0.0379	0.0006	0.3376	238	9.6	240	3.6	244	7.6
SD33-15	484	751	0.64	0.0527	0.0035	0.2575	0.0153	0.0365	0.0005	0.2412	233	12.3	231	3.2	247	8.9
SD33-16	760	1116	0.68	0.0512	0.0023	0.2618	0.0113	0.0371	0.0004	0.2557	236	9.1	235	2.6	232	6.8
SD33-17	500	810	0.62	0.0505	0.0027	0.2672	0.0141	0.0384	0.0009	0.4664	240	11.3	243	5.9	233	7.0
SD33-18	617	818	0.75	0.0511	0.0031	0.2566	0.0153	0.0366	0.0005	0.2245	232	12.3	232	3.0	230	6.8
SD33-19	433	673	0.64	0.0507	0.0030	0.2627	0.0153	0.0375	0.0006	0.2533	237	12.3	237	3.4	237	8.2
SD33-20	498	989	0.50	0.0509	0.0025	0.2685	0.0132	0.0380	0.0004	0.2389	241	10.5	241	2.8	249	7.5
SD33-21	326	579	0.56	0.0513	0.0037	0.2751	0.0195	0.0388	0.0006	0.2100	247	15.5	246	3.6	255	9.3
SD33-22	757	991	0.76	0.0504	0.0030	0.2608	0.0157	0.0375	0.0005	0.2000	235	12.7	237	2.8	227	7.6
SD33-23	986	1322	0.75	0.0507	0.0022	0.2540	0.0105	0.0363	0.0005	0.3245	230	8.5	230	3.0	221	6.4
SD33-24	380	678	0.56	0.0521	0.0030	0.2709	0.0151	0.0382	0.0005	0.2472	243	12.1	242	3.3	240	8.6
SD33-25	1227	1538	0.80	0.0505	0.0018	0.2632	0.0090	0.0376	0.0004	0.2951	237	7.2	238	2.4	232	5.6
SD33-26	627	970	0.65	0.0519	0.0028	0.2686	0.0140	0.0380	0.0005	0.2547	242	11.2	241	3.1	253	9.1
SD33-27	404	672	0.60	0.0509	0.0031	0.2680	0.0166	0.0385	0.0006	0.2556	241	13.3	243	3.8	233	8.4
SD33-28	517	817	0.63	0.0512	0.0027	0.2830	0.0152	0.0401	0.0006	0.2926	253	12.0	253	3.9	251	8.4
SD33-29	1624	1785	0.91	0.0511	0.0019	0.2726	0.0097	0.0385	0.0004	0.2997	245	7.7	244	2.6	231	5.5
SD33-30	401	667	0.60	0.0507	0.0032	0.2608	0.0161	0.0378	0.0006	0.2395	235	12.9	239	3.5	226	8.6

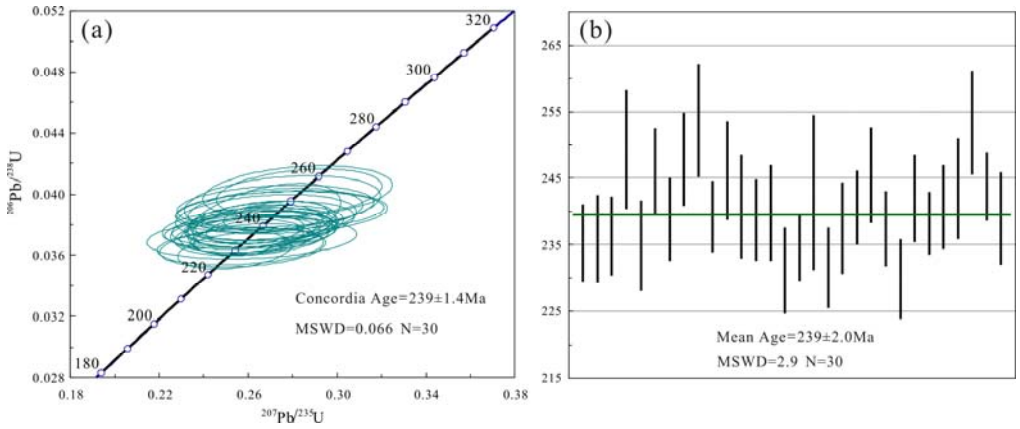

Figure 5.a) LA-ICP-MS U-Pb concordia diagrams, b) Weighted mean $^{206}Pb/^{238}U$ age for zircon of the Shadong granite samples

4.2 Major and Trace Elements

Major and trace elements results of analyzed samples are shown in Table 2, with SiO_2 in the range of 64.0–68.5wt.%, Al_2O_3 in the range of 14.6–16.1wt.%, K_2O+Na_2O in the range of 6.71–7.36wt.% and K_2O/Na_2O ratios of 0.73–0.96. The Rittman index is between 1.99 and 2.28, showing that these rocks belong to the calc alkaline series. From the K_2O-SiO_2 diagram (Fig. 6a), the studied samples belong to high-K calc-alkaline series. Aluminum saturation index (A/CNK ratio) are between 0.95 and 1.02 and A/CNK-A/NK diagram showed that the studied samples belong to metaluminous to slightly peraluminousrocks (Fig. 6b). Only foursamples include normative corundum of CIPW standard minerals, accounting for 0.10 – 0.64wt.% and the differentiation indexes (DI) of samples are between 69 and 80.

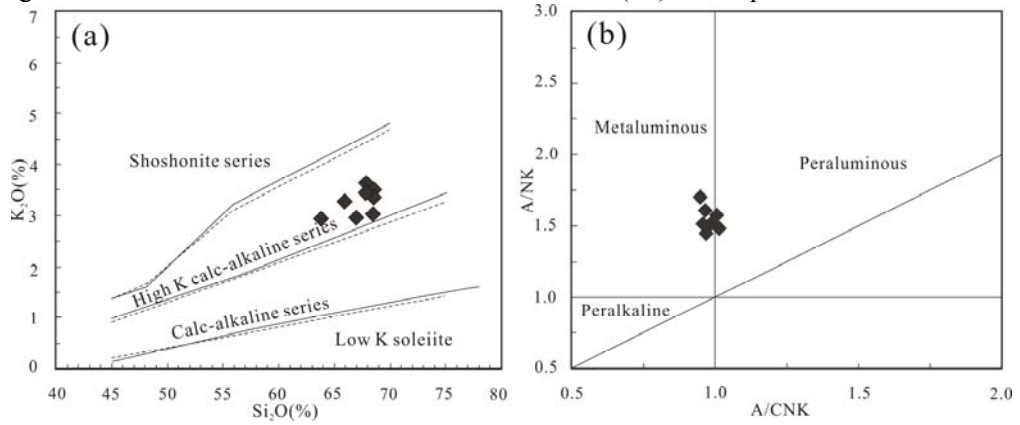

Figure 6.a)K_2O-SiO_2 diagram of Shadong granite samples (Peccerillo *et al*., 1976);b) A/NK-A/CNK diagram of Shadong granite samples (Rickwood , 1989)

Normalized spider of primitive mantle diagrams (Fig. 7a) showed that the samples are rich in large ion lithophile elements(LILE) such as K, Rb and Th, depleted in high field strength elements(HFSE) such as Nb, Ta, P and Ti, and slightly depleted in Sr and Ba. Total contents of rare earth elements(∑REE) of samples are between 135.36and 179.46ppm, of which LREE/HREE ratiosare between 11.74and 21.57, $(La/Yb)_N$ ratiosare between 16.29and 36.8, indicating a high Fractionationbetween lightand heavyrareearthelements.Chondrite-normalized REE patterns show the right-dipping(Fig. 7b). Eu/Eu*(Eu anomaly) are in the range of 0.71–0.82, indicating that the rock has the weak negative Eu anomaly.

Table 2 Major and trace elements compositions of Shadong granite samples

Sample number	SD-33	SD-34	SD-35	SD-36	SD-41	SD-42	SD-44	SD-47
Sample position	ZK5601 -690m	ZK5601 -720m	ZK5601 -870m	ZK5601 -945m	ZK8003 -660m	ZK8003 -720m	ZK8003 -780m	ZK0007 -1040m
Major element (wt.%)								
SiO_2	67.8	67.0	67.8	68.4	68.5	65.9	64.0	68.4
Al_2O_3	15.00	15.10	15.00	14.95	14.6	16.10	16.05	14.90
CaO	2.77	2.99	2.93	2.94	2.44	3.66	4.12	3.13
K_2O	3.45	2.96	3.61	3.01	3.46	3.28	2.83	3.36
Na_2O	3.74	3.95	3.75	3.99	3.70	3.94	3.88	3.77
MgO	1.69	1.54	1.45	1.44	1.28	1.70	2.32	1.42
Fe_2O_3	3.12	3.12	3.09	3.02	2.66	3.66	4.25	3.02
P_2O_5	0.14	0.14	0.13	0.13	0.12	0.18	0.21	0.13
TiO_2	0.46	0.46	0.44	0.43	0.41	0.58	0.65	0.43
MnO	0.06	0.05	0.06	0.05	0.04	0.06	0.07	0.05
LOI	1.06	2.10	1.37	0.86	2.08	0.97	1.15	1.20
Tatol	99.3	99.4	99.6	99.2	99.3	100.0	99.5	99.8
K_2O+Na_2O	7.19	6.91	7.36	7.00	7.16	7.22	6.71	7.13
K_2O/Na_2O	0.92	0.75	0.96	0.75	0.94	0.83	0.73	0.89
A/CNK	1.00	1.00	0.97	0.98	1.02	0.96	0.95	0.96
Trace element (ppm)								
Rb	240	253	184.0	181.0	183.0	224	211	161.0
Sr	343	333	318	318	327	373	420	313
Ta	0.8	0.8	0.9	0.9	0.7	0.8	1.1	0.9
Nb	8.6	8.9	8.6	9.1	7.5	9.2	8.3	7.7
Th	14.70	14.00	15.55	13.55	14.20	16.55	11.00	14.90
U	3.47	3.56	4.36	4.72	2.29	3.64	2.44	3.49
V	54	52	55	42	40	61	63	44
w	8	17	171	21	25	102	32	15
Zr	237	218	160	180	178	233	265	162
Ba	733	747	886	730	1090	729	779	1070
Ga	22.8	21.5	22.5	21.2	19.3	22.4	22.5	19.7
La	32.1	35.6	31.5	35.3	43.1	30.2	44.5	42.2
Ce	62.1	67.8	61.6	66.5	75.9	60.8	78.7	71.8
Pr	6.48	6.67	6.21	6.71	7.36	6.71	7.92	6.91
Nd	23.2	23.7	22.0	23.9	24.6	24.0	29.7	25.2
Sm	4.24	3.96	3.84	4.06	3.50	4.78	5.68	4.38
Eu	0.94	0.87	0.98	0.94	0.81	1.05	1.24	0.91
Gd	3.45	3.23	3.26	3.33	2.70	3.75	4.33	3.18
Tb	0.43	0.43	0.40	0.45	0.34	0.47	0.60	0.42
Dy	2.56	2.44	2.48	2.39	1.82	2.89	3.00	2.30
Ho	0.43	0.46	0.43	0.45	0.34	0.52	0.54	0.41
Er	1.30	1.23	1.24	1.28	0.89	1.49	1.52	1.16
Tm	0.20	0.17	0.19	0.20	0.13	0.21	0.21	0.16
Yb	1.11	1.14	1.04	1.23	0.84	1.33	1.32	1.13
Lu	0.18	0.17	0.19	0.20	0.14	0.20	0.20	0.13
Y	12.2	12.4	11.9	12.0	8.6	13.9	14.3	11.2
ΣREE	138.72	147.87	135.36	146.94	162.47	138.40	179.46	160.29
LREE/HREE	13.36	14.95	13.67	14.42	21.57	11.74	14.31	17.03
$(La/Yb)_N$	20.74	22.40	21.73	20.59	36.80	16.29	24.18	26.79
*Eu/Eu**	0.73	0.72	0.82	0.76	0.78	0.73	0.73	0.71

NOTE:LOI= loss of ignition

A/CNK = $(Al_2O_3)/(CaO+K_2O+Na_2O)$ molar ratio

ΣREE= sum(La+Ce+Pr+Nd+Pm+Sm+Eu+Gd+Tb+Dy+Ho+Er+Tm+Yb+Lu)

LREE/HREE=(La+Ce+Pr+Nd+Pm+Sm+Eu)/(Gd+Tb+Dy+Ho+Er+Tm+Yb+Lu)

$(La/Yb)_N = (La_{sample}/ Yb_{sample})/(La_{chondrite}/ Yb_{chondrite})$

Eu/Eu* is a measure of the Eu anomaly .$Eu/Eu^* = Eu_N/[(Sm_N) \times (Gd_N)]^{0.5.}$

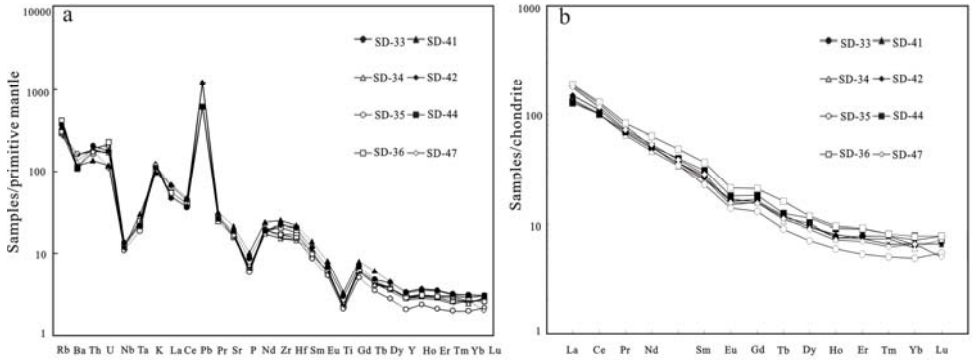

Figure7. a) Primitive mantle-normalized spider diagrams, b) Chondrite-normalizedREE patterns of Shadong granite samples

4.3 Whole-rock Sr-Nd isotopes

Sr-Nd isotope analysis results of studied granite samples are shown in table 3. Calculated with the age of 239.5Ma, ($^{87}Sr/^{86}Sr$)i ratios are between 0.70659–0.70775, $\varepsilon_{Nd(t)}$ values are between -1.77 and -2.53, depleted mantle Nd model ages (T_{DM1}) are between 0.97–1.30Ga, with the average age of 1.13Ga, and $T_{DM2}$are between 1.17–1.22Ga, with the average age of 1.18Ga.

4.4 Zircon in-situ Hf isotope

Hf isotope analyses of zircon are shown in Table 4. $^{176}Lu/^{177}Hf$ ratio is between 0. 000464 and 0.001272, which indicated that the radiogenic Hf is not accumulated after the zircon is formed and $^{176}Lu/^{177}Hf$ ratio measured is assumed to represent Hf isotope composition of the system during the formation of rocks (Knudsen et al., 2001; Gao, et al., 2015). $^{176}Hf/^{177}Hf$ ratios of 20 testing points are between 0.282702 and 0.282764, with average ratio of 0.282737. εHf(t) between 2.54 and 4.90 while the averagevalue of 3.84 were obtained through the correction computing of in situ age of zircon LA-ICP-MS dating. One-stage Hf model ages (T_{DM1}) are between 0.69 and 0.78Ga, with the average age of 0.73Ga. Two-stage Hf model ages (T_{DM2}) are between 0.87 and 0.98Ga, with the average age of 0.92Ga.

5 DISCUSSIONS

5.1 Granite type and magmatic source

Studied samples have the relatively low contents of SiO_2 (64.0–68.5wt.%) and the K_2O/Na_2O ratios are all less than 1. The contents of normative corundumare low(0.10 – 0.64 wt.%) and allthe samples aremetaluminous to slightly peraluminous (A/CNK ratios=0.95–1.02). The above features are all conformed to I-type granitic characteristics (Chappell and White 1992; Chappell, 1999; Frost et al., 2001). Compared with aluminum saturation index (A/CNK), the P_2O_5 content in granite is the more reliable index to identify the genetic type of granite (Wu et al., 2003; Broska et al., 2004; Li et al., 2007; Zhouet al., 2016). Samples have the low content of P_2O_5 (0.13–0.21wt.%). As shown in Figure 9, P_2O_5 and SiO_2 have the negative correlation, showing the feature of I-type granite(Fig. 8a). Moreover, the K_2O-Na_2O diagram of granite showed that samples all belong to I-type granite (Fig. 8b).

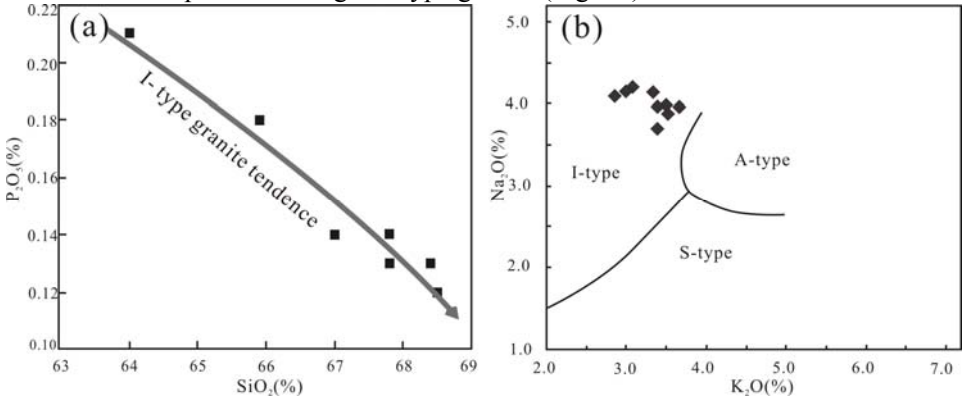

Figure8.P_2O_5-SiO_2 diagram(a)and K_2O-Na_2O diagram(b) of Shadong granite samples (Collins, 1982)

Table 3 Whole rock Sm-Nd isotopic compositions of Shadong granite samples

Sample number	Sm (ppm)	Nd (ppm)	$^{147}Sm/^{144}Nd$	$^{143}Nd/^{144}Nd$	2σ	$\varepsilon_{Nd}(0)$	$\varepsilon_{Nd}(t)$	T_{DM1} (Ma)	T_{DM2} (Ma)	Rb (ppm)	Sr (ppm)	$^{87}Rb/^{86}Sr$	$^{87}Sr/^{86}Sr$	2σ	$^{87}Sr/^{86}Sr(t)$
SD-33	4.24	23.2	0.115	0.51242	0.000005	-4.25	-1.77	1131	1158	240	343	1.97	0.714043	0.000013	0.70733
SD-41	3.5	24.6	0.089	0.512363	0.000006	-5.36	-2.10	969	1185	183	327	1.58	0.713119	0.000010	0.70775
SD-42	4.78	24	0.125	0.512397	0.000006	-4.70	-2.53	1303	1220	224	373	1.69	0.713059	0.000008	0.70730
SD-47	4.38	25.2	0.109	0.512401	0.000005	-4.62	-1.96	1098	1174	161	313	1.45	0.711527	0.000006	0.70659

Table 4 Zircon Hf isotopic compositions of Shadong granite samples

Sample number	$^{176}Hf/^{177}Hf$	1σ	$^{176}Lu/^{177}Hf$	1σ	$^{176}Yb/^{177}Hf$	1σ	εHf(0)	1σ	εHf(t)	1σ	T_{DM1}(Ma)	T_{DM2}(Ma)	$f_{Lu/Hf}$	t (Ma)
SD33-1	0.282751	0.000011	0.000665	0.000023	0.017504	0.000683	-0.7	0.7	4.4	0.7	735	932	-0.97	235
SD33-2	0.282755	0.000012	0.001023	0.000035	0.026626	0.001034	-0.6	0.7	4.5	0.7	738	940	-0.98	236
SD33-3	0.282752	0.000010	0.000764	0.000013	0.018721	0.000348	-0.7	0.6	4.4	0.6	751	953	-0.97	236
SD33-4	0.282749	0.000012	0.000975	0.000013	0.025330	0.000405	-0.8	0.7	4.3	0.7	768	972	-0.96	249
SD33-5	0.282749	0.000013	0.001198	0.000026	0.030379	0.000689	-0.8	0.7	4.3	0.7	777	992	-0.97	235
SD33-6	0.282753	0.000012	0.000827	0.000022	0.021434	0.000635	-0.7	0.7	4.5	0.7	727	915	-0.96	246
SD33-7	0.282719	0.000011	0.000896	0.000013	0.021746	0.000354	-1.9	0.7	3.2	0.7	726	919	-0.97	239
SD33-8	0.282764	0.000010	0.000862	0.000005	0.022190	0.000169	-0.3	0.6	4.8	0.6	749	953	-0.97	248
SD33-9	0.282763	0.000013	0.001004	0.000024	0.026254	0.000561	-0.3	0.7	4.8	0.7	741	949	-0.99	254
SD33-10	0.282760	0.000014	0.001030	0.000015	0.026713	0.000326	-0.4	0.7	4.7	0.7	769	985	-0.98	239
SD33-11	0.282732	0.000011	0.000890	0.000031	0.021754	0.000831	-1.4	0.6	3.7	0.7	703	892	-0.98	246
SD33-12	0.282727	0.000011	0.000721	0.000006	0.017542	0.000186	-1.6	0.6	3.6	0.7	704	887	-0.97	241
SD33-13	0.282722	0.000011	0.000987	0.000012	0.024689	0.000290	-1.8	0.6	3.3	0.7	704	891	-0.98	239
SD33-14	0.282714	0.000013	0.001272	0.000020	0.032883	0.000530	-2.1	0.7	3.0	0.7	713	900	-0.97	240
SD33-15	0.282702	0.000011	0.000850	0.000016	0.020716	0.000364	-2.5	0.7	2.6	0.7	717	902	-0.96	231
SD33-16	0.282743	0.000012	0.001302	0.000098	0.034639	0.002686	-1.0	0.7	4.0	0.7	704	890	-0.98	235
SD33-17	0.282739	0.000012	0.000926	0.000029	0.023906	0.000739	-1.2	0.7	3.9	0.7	753	958	-0.97	243
SD33-18	0.282721	0.000016	0.000854	0.000014	0.021697	0.000348	-1.8	0.8	3.3	0.8	689	869	-0.97	232
SD33-19	0.282722	0.000011	0.000464	0.000046	0.010978	0.001327	-1.8	0.6	3.4	0.7	692	871	-0.97	237
SD33-20	0.282704	0.000009	0.000647	0.000036	0.016216	0.000975	-2.4	0.6	2.8	0.6	697	877	-0.97	241

The samples are rich in K, Rb and Th but depleted in Nb, Ta, Ti and P, indicating that the magmatic source had been subject to the contamination and metasomatism of crustal components(Ryerson et al., 1987; Liu et al., 2017). Nb/Ta ratio can represent the proportion of crustal components when the magma was formed (Pfänder et al., 2007; Stepanov and Hermann, 2013). In this research, Nb/Ta ratios of samples are in the range of 7.55–11.12, which are between lower crust (8.3) and depleted mantle (17.5) (Sun et al., 1989), showing the characteristic of crust-mantle mixed source. Research suggests that Sr content and Eu anomaly can indicate the forming depth of granite body(Zhang et al., 2010, 2011). The samples are slightly depleted in Sr (313–420ppm) with weak Eu negative anomaly. This feature is between that of Adakite (Sr>400ppm, without Eu negative anomaly or positive Eu anomaly) which was formed by partial melting of the thickening lower crust in East Tianshan (Castillo, 2006; Wang et al., 2015) and the crust-originated granite (Sr content is low with strong Eu negative anomaly) which was formed by partial melting of shallow crust (Visona et al., 2002; Zhang et al., 2011). Above comparison showed that Shadong granite mass may be formed in the middle crust between them. It is generally considered that Sr and Eu negative anomaly are caused by the fractional crystallization of plagioclase (Drummond and Defant, 1990; Mei et al., 2014). Differential degree of Shadong granite is not high and a considerable content ofplagioclase exist in granite, therefore, Sr and Eu negative anomaly shall not be caused by the fractional crystallization of plagioclase but by a few residual plagioclase in source region(zhang et al., 2011). In addition, MREE of study samples has the differentiation, which is generally caused by fractional crystallization of hornblende (Schmidt, 1992; Foley et al., 2002). Eu-Yb and Sm-Yb diagram also reflect the fractional crystallization of hornblende (Fig. 9), indicating that residual hornblendes exist in source region, while HREE loss of study samples imply that garnet (or pyroxene) should exist in source region (Stevens et al., 2007; Zhang et al., 2011). Therefore, the residual phases of source rock of the granite are amphibolites facies or amphibolites-granulite facies, which should be located in the depth of the middle crust (Xiong et al., 2005). In study area, Xingxingxia Group of Mesoproterozoic Changcheng system has the above-mentioned characteristic and could be the crustal components of Shadong granite magma(Hu et al., 2000, 2006).

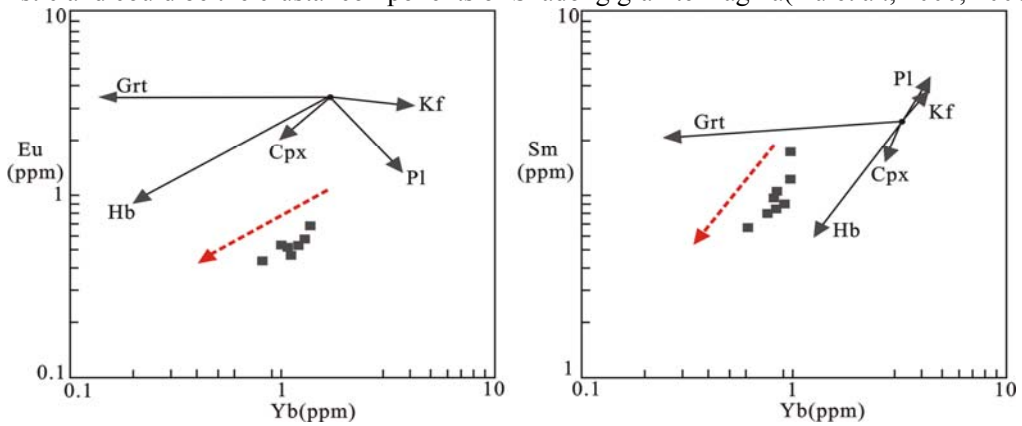

Figure9. Simulated Diagram of Fractional Crystallization of Shadong granite samples

Cpx–monoclinic pyroxene; Hb–hornblende; Kf–potassium feldsparp; Pl–plagioclase;Grt–garnet

(minerals/melt distribution coefficient referring to Rollinson (1993); Rayleigh equation for simulation referring to Li,(1992))

Sr and Nd isotopes of whole rock and Hf isotope of zircon can effectively indicate the magma source of the granite(Xinget al.,2016, Zhaoet al.,2016). The ($^{87}Sr/^{86}Sr$)i ratios are between 0.70659–0.70775, which are relatively low and generally belong to the range of I type granite(Keay et al., 1997).εNd(t)-t diagram (Fig.10a) shows that all samples are located between Proterozoic continental crust in East Tianshan area and young crust in north Xinjiang, with low Nd model age, while εHf(t)-t diagram (Fig. 10b) indicates that all the samples are situated above the Hf isotope crustal evolution line, with low Hf model age. The above results both reveal that the magma sourceof Shadong granite may include mantle material(Teixeira et al., 2011; Wang et al., 2011; Liu et al., 2012). In addition, $\delta Eu\text{-}(La/Yb)_N$ diagram also

shows that all samples belong to crust-mantle mixed source (Fig. 10c) (Hu et al., 2013).The binary mixing simulation based on Nd isotope compositioncan be used to estimate the proportion of mantle derived magma (DePaolo, et al.,1992; Jahn et al., 2000a). Xingxingxia Groupis widely exposed around the study area, which is one of the potential sources of Shadong granite and can be regarded as the crustal end member in this region(Hu et al., 2000, 2006). Moreover, the εNd(t) values of the Indosinian basite and lamprophyre in east Tianshan area are all positive（1.0–4.2）, showing the characteristics of the depleted mantle(Han et al., 1999; Jahn et al., 2000b; Wang et al., 2008;). Therefore, we choose the Nd isotopic composition of Paleozoic ophiolite in this region as the approximate depleted mantle end member.Thecalculation method can be seen fromJahn et al., (2000a). Simulation results show that the proportion of mantle source components in four samples are between 58% and 60%(Fig. 10d). Based on the above judgment for the rock mass resource, we considered that the mixing of mantle derived magma and middle crust materials are the most possible sources of Shadong granite, while the Mesoproterozoic Xingxingxia Group with metamorphic grade of hornblende facies and hornblende granulite facies, should be the source of crustal components.

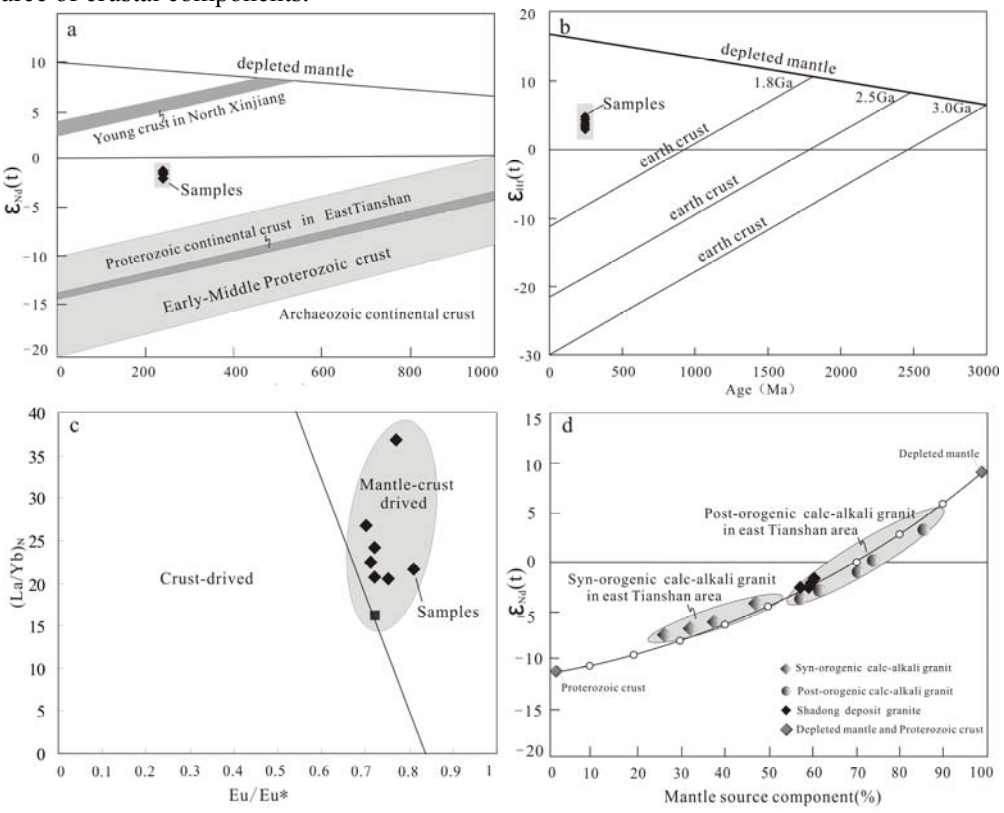

Figure10. Source region component diagram of Shadong granite samples

a) $\varepsilon_{Nd(t)}$-tdiagram of Shadong granite samples.Proterozoic continental crust evolution line is drawn by the data from Hu *et al*., (2006)Young crust of north Xinjiang evolution line is drawn by the data from Han *et al*., (1999),b) $\varepsilon_{Hf(t)}$-tdiagram of Shadong granite samples (from Mao *et al*., 2010),c) δEu-$(La/Yb)_N$ diagram of Shadong granite samples (from Hu *et al*., 2013),d) Proportion estimation diagram of mantle source component of Shadong granite samples$X^m=(\varepsilon^c-\varepsilon^t)Nd_c/[\varepsilon^t(Nd_m-Nd_c)-(\varepsilon^m Nd_m-\varepsilon^c Nd_c)]$ (DePaolo, *et al*.,1992; Jahn 2000 *et al.*); X^m= Mantle source proportion; Nd_c , Nd_m= Nd content in the crust and mantlerespectively; ε^c , ε^t, ε^m= Nd isotope composition of crust, samples in this study and mantlerespectively;Nd_m=15 (from Jahn *et al*., 2000a) ,ε^m=+9.5; Nd_c=25; ε^c=–12 (recalculated by the data from Hu *et al*., 2000; Wang *et al*., 2008).

5.2 Tectonic setting of Shadong granite and indication for crustal growth

A lot of studies showed that East Tianshan Orogenic Belt gradually entered the post-orogenic stage after early Permian and entered the intraplate tectonic setting after the early Triassic (Gu et al., 2006;

Klemd et al., 2011; Chen et al., 2013, Xiao et al., 2014;Wang et al., 2016; Wu et al., 2017). In this research, theintrusive age of Shadong granite is 239±2.0Ma, belonging to the Middle Triassic. From the perspectiveof age, the magmaof Shadong granite should bederived from the magmation in post-orogenic stage. In R1-R2 and Rb/30-Hf-3Ta discrimination diagram (Betchelor, 1985), The granite samples are situated in the area of post-orogenic and intraplate tectonic setting, which is consistent with the conclusions of previous research.

The magma sources of Shadong graniteincludemantle derived magma according to the above discussion. It is a general characteristic that magmatic source of granites in Central Asian orogenic belt include young mantle components, showing the growth of the Phanerozoic continental crust(Jahn et al., 2000a, b; Hu et al., 2000; Wu et al., 2000; Hong et al., 2004). There are two approaches for continental crust growth: horizontal growth and vertical growth. The mantle-derived materials of synorogenic (such as subduction stage) granites with high εNd(t) or εHf(t) valuesare mainly from oceanic crust, showing the horizontal growth(Xiao et al., 2013, 2014); while mantle-derived components of post orogenic granites with high εNd(t) or εHf(t) values are very complex(Petford et al., 2000; Wang et al., 2005; Wang et al., 2016). Generally speaking, the young material source of post-orogenic granites has at least three possibilities: 1. New mantlederived magma by underplating and intraplating; 2. The oceanic crust or young volcanic arc left in continentalcrust; 3. The juvenile lower crust transformed by the underplating basic magmas in the Proterozoic Era(Albarde, 1998; Condie, 1998; Wang et al., 2005). We considered that the first case is more likely for the follow reasons:

(1) No obvious subduction sign were found at the southern margin of Central Tianshan massifaround Shadong mining area, for instance, no obvious subduction zone(Jahn et al., 2004; Su et al., 2012). There are ophiolites distributed along the Hongliu river at the southern margin of Central Tianshanmassif, which should be formed in back-arc basin environment, without strong deformation band in the surrounding place (Li et al., 2001; Guo et al., 2006). It indicated that there are few oceanic crustal slices inserted or left in crust.

(2) The dynamical mechanism of plate subduction and collision had been finished in late Paleozoic in east Tianshan area(Klemd et al., 2011; Xiao et al., 2014), so the formation of post-orogenic magma must have new geodynamics and heat source. Underplatingand intraplatingof mantlederived magma are the most common heat source and matter source of post orogenic magma(Wickham et al., 1996; Kovalenko et al., 2004). A lot of mafic dikes especially lamprophyre veins formed in late Paleozoic-early Mesozoic were developed around Shadong ore district and other areas in Central Tianshan massif, which provided the evidence (Zhang et al., 2005b; Wang et al., 2008; Jiang et al., 2012).

(3) Nd and Hf average model age of Shadong granite body are 0.92 and 1.18Ga respectively, belonging to Neoproterozoic. However, the diabase and lamprophyre vein in this region which were formed in the same period with the granite also have the Neoproterozoic Nd model age (Wang et al., 2008). It is indicated that either the granites or mafic dikes were mixed by the crust, thus had the lager impact on Nd model age. In this case, the Nd model age only shows the average mixed age without the definite geological significance (DePaolo et al., 1992; Murphy and Nance, 2002; Zhang et al., 2016). Thus the Nd and Hf isotope model age in this study can not be the evidence to prove that the underplating of mantle derivedmagma in the Neoproterozoic was transformed into juvenile lower crust in East Tianshan Orogenic Belt(Hu et al., 2000; He et al., 2014).

Crust-mantle interaction commonly exist in post orogenic and intraplateextension stage(Cunningham et al., 2003; Wang et al., 2008; Xiong et al., 2016). In consideration of the above evidences and the residual phases of the source rock of Shadong granite, we consider thatthe magma mixing during intraplating of mantle derived magma toward the Xingxingxia Groupof MesoproterozoicChangcheng Systemis the major formation mechanism of Shadong granite, providing a evidence for vertical accretion

of continental crust of east Tianshan area in the Indosinian Period.

5.3 Relationship with tungsten mineralization

A number of Indosinian diagenetic and metallogenic ages of tungsten and molybdenum deposits have been reported in recent years, indicating that the Indosinian mineralization is developed in East Tianshan Orogenic Belt(Lü et al., 2012; Wu et al., 2013; Zhu et al., 2013). Therein, The ore-forming porphyry ofmolybdenum depositsareconsidered to be formed the partial melting of juvenilelower crust caused by the mantle underplating (Wang et al., 2015;Wang et al., 2016; Wu et al., 2017). However, In consideration of the content of tungsten element in the crust, whether the partial melting of lower crust can form the large-scale magmatic hydrothermal type tungsten deposit is doubtful (Liu and Ma, 1987). It is generally considered that the granite magma geneticallyrelated to tungsten mineralization formed from partial melting of upper crust or the Precambrian metamorphosed basement in middle crust(Lu et al., 1993; Wang, 2005; Wei et al., 2006). Huet al. (2006) obtained that the tungstencontent of granitic gneiss of Xingxingxia Group of Changcheng System in Baluntai Region reaches 94 ppm, while in Xingxingxia Region of East Tianshan is generally greater than the tungsten content of average abundance in the crust (2.87–3.53 ppm) .Chen (2013) pointed out that the Xingxingxia Group of MesoproterzoicChangcheng System play an important role in the origin of tungsten ore in East Tianshan Orogenic Belt, and the tungsten deposits found in this region are mainly located around the above-mentioned Precambrian basement. Meanwhile,the ore-forming granites of Xiaobaishitou and Hongjianbingshan tungsten ore, which are formed inIndosinian epoch this region(Fig.1b), weremainly derived from partial melts from the tungsten-rich Xingxingxia Group or involving some mantle components (Nie et al., 2004; Li et al., 2005; Chen, 2013;Deng et al., 2017). It indicates that during the rising of the mantle-derived magma, the mixing of it with the wall rocks of middle crust(Xingxingxia Group) may be the reason of enrichment of tungsten element(Chen, 2013). The magmatic mixing is consistent with the origin of Shadong concealed granite body, indicating the tungsten-rich Xingxingxia Group of Changcheng System is supposed to provide the main metal source of Shadong tungsten ore. Further more, it is worth noting that many literatures reported the mantle-derived magma (fluid) played an important role in tungsten mineralization(Nie et al., 2004; Jiang et al., 2006; Xi et al., 2007; Zhai et al., 2012). Whether mantle-derived magma makes a contribution to Shadong tungsten mineralization is worthy of further exploration.

6CONCLUSIONS

The following conclusions were obtained through the analysis above:

1. Zircon U-Pb age of concealed granite body in Shadong tungsten deposit is 239±2.0 Ma, which is identified as Middle Triassic.

2. The lithogeochemistry and Sr-Nd-Hf isotopiccharacteristics revealedthat the concealed granite body in Shadong tungsten deposit is I-type granite, and occurred in anintraplate tectonic setting in East Tianshan Orogenic Belt. The magma mixing during intraplating of mantle derived magma toward the Xingxingxia Group of MesoproterozoicChangcheng Systemis the major formation mechanism of the Shadong granite,and the tungsten-rich Xingxingxia Group is supposed to provide the main source of ore forming metals of Shadong tungsten deposit.

ACKNOWLEDGMENTS

This study was financially supported by the project of Metallogical condition research and ore prospecting target area evaluation of copper-gold-iron metallogenic belt in Kuruktag (2011BAB06B04). We appreciate the engineers of Shadong deposite for their help and fruitful discussion during our field investigations.Comments and suggestions fromreviewers greatly improved the quality of thepaper.

REFERENCES CITED

Albarde, F., 1998. The growth of continental cryst. *Tectonophysics*, 296: 1–14. doi: 10.1016/S0040-1951(98)00133-4

Batchelor, R.A., and Bowden,P. 1985. Petrogenetic interpretation of granitoids series using multicationic parameters.*Chemical Geology*,48:43–55. doi: 10.1016/0009-2541(85)90034-8

Broska, I., Williams, C.T. and Uher, P., 2004. The geochemistry of phosphorus in different granite suites of the western Carpathians, Slovakia: the role of apatite and P-bearing feldspar. *Chemical Geology*, 205: 1–15. doi: 10.1016/j.chemgeo.2003.09.004

Collins, W.J. , 1982. Nature and origin of A type granites with paticular reference toSoutheastern Australia.*Contributions to Mineralogy and Petrology*, 80: 189–200. doi:10.1007/BF00374895

Chappell, B.W. and White, J.R., 1992. I-and S-type granites in the Lachlan Fold Belt. *Transactions of the Royal Society of Edinburgh: Earth Sciences*, 83(1-2): 1–26. doi: 10.1017/S0263593300007720

Condie, K.C., 1998. Episodic continental growth and supercontinents: a mantle avalanche connection? *Earth and Planetary Science Letters*, 163: 97–108. doi: 10.1016/S0012-821X(98)00178-2

Chappell, B.W., 1999. Aluminium saturation in I-and S-type granites and the characterization of fractionated hapogranites. *Lithos*, 46: 535–551.doi:10.1016/S0024-4937(98)00086-3

Cunningham, D., Owen, L.A., Snee, L.W. and Li, J.L., 2003. Structural framework of a major intracontinental orogenic termination zone, the easternmost Tien Shan, China. *Journal of the Geological Society, London* 160: 575–590.doi: 10.1144/0016-764902-122

Castillo, P.R., 2006. An overview of adakite petrogenesis. *Chinese Science Bulletin*,51: 257–268.doi: 10.1007/s11434-006-0257-7

Chen, C., Lü, X.B., Cao, X.F. and Wu, C.M., 2013a.Geochronology, geochemistry and geological significance of late Carboniferous-early Permian granites in Kumishi area,Xinjiang,*Earth Science-Journal of China University of Geosciences* ,38: 218–232 (in Chinese with English abstract)

Chen, C., 2013b. Tungsten mineralization study of East Tianshan-Beishan area:[Dissertation]. China University of Geoscience(Wuhan), 170 (in Chinese with English abstract)

Drummond, M.S. and Defant, M.J., 1990. A model for trondhjemite-tonalite-dacite genesis and crustal growth via slab melting: archean to modern comparison. *Journal of Geophysics Research*, 95: 21503–21521.doi: 10.1029/JB095iB13p21503

DePaolo, D.J., Perry, F.V. and Baldridge, W.S., 1992. Crustal versus mantle sources of granitic magmas: a two-parameter model based on Nd isotopic studies. *Transactions of the Royal Society of Edinburgh: Earth Sciences*, 83: 439–446.

Dong, Y.P., Zhang, G.W. and Neubauer, F., 2011. Syn-and post-collisional granitoids in the Central Tianshan orogen: geochemistry, geochronology and implications for tectonic evolution. *Gondwana Research*, 20: 568–581. doi:10.1016/j.gr.2011.01.013

Deng, X.H., Chen, Y.J., Santosh, M., et al., 2017. U–Pb zircon and Re–Os molybdenite geochronology from theXiaobaishitou W(−Mo) deposit: implications for Triassic tectonic setting in easternTianshan, NW China. *Ore Geology. Review*, 80: 332–351.doi: 10.1016/j.oregeorev.2016.05.013

Frost, B.R., Barnes, C.G. and Collins, W.J. 2001. A geochemical classification for granitic rocks. *Journal of Petrology*,42: 2033–2048.doi: 10.1093/petrology/42.11.2033

Foley, S., Tiepolo, M. and Vannucci, R. , 2002. Growth of earth continental crust controlled by melting of amphibolites in subduction zones. *Nature*,417: 837–840. doi: 10.1038/nature00799

Guo, Z.J., Shi, H.Y., Zhang, Z.C., et al., 2006. The tectonic evolution of the south Tianshan paleo-oceanic crust inferredfrom the spreading structures and Ar-Ar dating of the Hongliuhe ophiolite, NW China. *Acta Petrlologica Sinica*, 22: 95–102 (in Chinese with English abstract)

Gu, L.X., Zhang, Z.Z., Wu, C.Z., et al.,2006. Some problems on granites and vertical growth of the continental crust in the eastern Tianshan Mountains. NW China.*Acta Petrologica Sinica*,22:

1103–1120 (in Chinese with English abstract)

Gao, Q.L., Chen, Z.Q., Zhang, N., et al., 2015.Ages, Trace Elements and Hf-Isotopic Compositions of Zircons from Claystones around the Permian-Triassic Boundary in the Zunyi Section, South China: Implications for Nature and Tectonic Setting of the Volcanism.*Journal of Earth Science*, 26(6):872–882.doi: 10.1007/s12583-015-0589-9

Hu, A.Q., Zhang, J.B., Zhang, Z.G. et al., 1982. Study on thermal history of Tianshan geosyncline, based on K-Ar age of eastern Tianshan. *Science in China (Ser.B)*, 25: 1214–1226 (in Chinese with English abstract)

He, Z.Y., Zhang, Z.M., Zong, K.Q.,et al.,2014. Zircon U-Pb and Hf isotopic studies of the Xingxingxia complex from eastern Tianshan (NW China): significance to the reconstruction and tectonics of the southern Central Asian Orogenic Belt. *Lithos*, (190–191): 485–499. doi:10.1016/j.lithos.2013.12.023

Han, B.F., He, G.Q. and Wang, S.G., 1999. Postcollisional mantle-derived magmatism, underplating and nature of basement of Junggar. *Science in China (series D)*, 29: 16–27. doi: 10.1007/BF02878509

Hu, A.Q., Jahn, B.M., Zhang, G.X., et al., 2000. Crustal evolution and Phanerozoic crustal growth in northern Xinjiang: Nd isotopic evidence, Part I.Isotopic characteristics of basement rocks. *Tectonophysics*, 328: 15–51. doi: 10.1016/S0040-1951(00)00176-1

Hidaka, H., Shimizu, H. and Adachi, M., 2002. U-Pb geochronology and REE geochemistry of zir cons from Palaeoproterozoic paragneiss clasts in the Mesozoic Kamiaso conglomerate, central Japan: evidence for an Archean provenance. *Chemical Geology*,187: 278–293. doi:10.1016/S00 09-2541(02)00058-X

Hong, D.W., Wang, S.G., Xie, X.L., et al.,2004. Continental crustal growth and the supercontinental cycle: evidence from the Central Asian Orogenic Belt. *Journal of Asian Earth Sciences*, 23: 799–813. doi: 10.1016/S1367-9120(03)00134-2

Hu, A.Q., Zhang, G.X., and Chen, Y.B., 2006. Isotope geochronology and geochemistry for major geological events of continental crustal evolution of Xinjiang, China. Beijing, Geological Publishing House. 421 (in Chinese)

Hu, Z.C., Liu, Y.S., Gao, S., Liu, W.G., et al., 2012. Improved in situ Hf isotope ratio analysis of zircon using newly designed X skimmer cone and Jet sample cone in combination with the addition of nitrogen by laser ablation multiple collector ICP-MS. *Journal of Analytical Atomic Spectrometry*,27: 1391–1399. doi: 10.1039/c2ja30078h

Hu, S.Q., Zhu, Q., Zhang, X.J., et al.,2013.Geochronology, geochemistry and zircon Hf isotope of granite porphyry in Yuanzhuding Cu-Mo deposit, Guangdong Province.*Mineral deposites*, 32: 1139–1158 (in Chinese with English abstract)

Jahn, B.M., 1999. Sm-Nd isotope tracer study of UHP metamorphic rocks: implications for continental subduction and collisional tectonics.*International Geology Review*, 41: 859–885. do i: 10.1080/00206819909465175

Jahn, B.M., Wu, F. and Hong, D., 2000a. Important crustal growth in the Phanerozoic: isotopic evidence of granitoids from east-central Asia. *Proc,Indian Acad. Sci.(Earth Planet Sci.)*,109: 5–20. doi: 10.1007 /BF02719146

Jahn, B.M., Wu, F. and Chen, B., 2000b. Masssive granitoid generation incentral Asia: Nd isotopic evidence and implication for continental growth in the Phanerozoic. *Episodes* 23: 82–92

Jahn, B.M., Windley, B.F., Natal'in, B.,et al.,2004.Phanerozoic continental growth in Central Asia-Preface. *Journal of Asian EarthSciences*,23:599–603. doi: 10.1016/S1367-9120(03)00124-X

Jiang, S.H. and Nie, F.J., 2006. ^{40}Ar-^{39}Ar geochronology of Hongjianbingshan tungsten deposit in Beishan Mountain, Gansu Province, China. *Mineral Deposits*, 25: 89–94 (in Chinese with English abstract)

Jiang, X., Guo, Y.M., Yang, L.Z., et al., 2012.Geological characteristics and preliminary origin of Shadong

large tungsten deposit in Hami, Xinjiang.*Xinjiang Geology*, 30: 31–35 (in Chinese with English abstract)

Keay, S., Collins, W.J. and McCulloch, M.T., 1997. A three component Sr-Nd isotopic mixing mo del for granitoid genesis, Lachlan fold belt eastern Australia. *Geology*, 25: 307–310. doi: 10.1 130/0091-7613(1997)025<0307:ATCSNI>2.3.CO;2

Knudsen, T.I., Griffin, W.I., Hartz, E.H., et al.,2001. In situ hafnium and lead isotope analyses of detrital zircons from the Devonian sedimentary basin of NE Greenland: a record of repeated crustal reworking. *Contributions to Mineralogy and Petrology*, 141: 83–94

Kovalenko, V.I., Yarmolyuk, V.V., Kovach, V.P., et al., 2004. Isotope provinces, mechanisms of generation and sources of the continental crust in the Central Asia mobile belt: geological and isotopic evidence. *Journal of Asian EarthSciences*, 23: 605–627. doi: 10.1016/S1367-9120(03)00130 -5

Kröner, A., Hegner, E. and Lehmann, B. , 2008. Palaeozoic arc magmatism in the Central Asian Orogenic Belt of Kazakhstan: SHRIMP zircon ages and whole-rock Nd isotopic systematics. *Journal of Asian Earth Science*, 32: 118–130. doi: 10.1016/j.jseaes.2007.10.013

Klemd, R., John, T., and Scherer, E.E., 2011. Changes in dip of subducted slabs at depth: petrological and geochronological evidence from HP-UHP rocks (Tianshan NW-China). *Earth and Planetary Science Letters*, 310: 9–20. doi: 10.1016/j.epsl.2011.07.022

Liu,Y.J. and Ma, D.S. ,1987. Geochemistry of tungsten. Beijing, Science Press, 232 (in chinese)

Li, C.N., 1992. Trace elements petrology of igneous rock. Wuhan, China University of Geosciences Publishing, 195 (in Chinese)

Lu, H.Z., 1993. Tungsten mineralization of South China.Beijing, Geological Publishing House, 232 (in Chinese)

Li, W.P., Wang, T., Li, J.B., Kang, X. et al., 2001. Geochemical characteristics and tectonic setting of the late Paleozoic granites from the Hongliuhe area, eastern Tianshan. *Geological Review*,47: 368–376 (in Chinese with English abstract)

Ludwig, K.R., 2003. ISOPLOT 3.0: A Geochronological Toolkit forMicrosoft Excel, Berkley Geochronology Center. Special publicationNo. 4

Li, H.Q., Chen, F.W., Lu, Y.F., et al., 2005. New chronological evidence for Indosinian diagenetic mineralization in eastern Xinjiang, NW China. *Acta Geologica Sinica*,79: 264–275. doi:10.33 21/j.issn:1000-9515.2005.02.012

Li, X.H., Li, Z.X., and Li, W.X., 2007.U-Pb zircon, geochemical and Sr-Nd-Hf isotopic constraint s on age and origin of Jurassic I- and A-typegranites from central Guangdong, SE China: a major igneous event in response to foundering of a subducted flat-slab? *Lithos*, 96:186–204. d oi:10.1016/j.lithos.2006.09.018

Liu, Y.S., Hu, Z.C. and Gao, S., 2008. In situ analysis of major and trace elements of anhydrous minerals by LA-ICP-MS without applying an internal standard. *Chemical Geology*,257: 34–43. doi: 10.1016/j.chemgeo.2008.08.004

Liu, Y.S., Hu, Z.C. and Zong, K.Q., 2010. Reappraisement and refinement of zircon U-Pb isotope and trace element analyses by LA-ICP-MS. *Chinese Science Bulletin*, 55: 1535–1546. doi:10.1007/s1143 4-010-3052-4

Liu, W., Liu, X.J. and Xiao, W.J., 2012. Massive granitoid production without massive continental-crust growth in the Chinese Altay: insight into the source rock of granitoids using integrated zircon U-Pb age, Hf-Nd-Sr isotopes and geochemistry. *American Journal of Science*,312: 29–84. doi:10.2475/06.2012.02

Lü, X.B., Zhu J., Cao, X.F., Chen, C., et al., 2012. Magmatism and its metallogenetic effects during the

Paleozoic-Triassic continental crustal constructionin the Liuyuan Area, South Beishan, NW China.*Geological Science and Technology Information*, 31: 119–127 (in Chinese with English abstract)

Li, D.P., Du, Y.S., Pang, Z.S., et al.,2013. Zircon U-Pb chronology and geochemistry of Carboniferous volcanic rocks in Awulale area, Western Tianshan Mountains.*Acta Geoscientica Sinica*, 34: 176–192 (in Chinese with English abstract)

Liu, M., Zhao, H.T., Zhang, D. et al., 2017. Chronology, Geochemistry and Tectonic Implications of Late Palaeozoic Intrusions from South of Xiwuqi, Inner Mongolia. *Earth Science*,42(4): 527–548 (in Chinese with English abstract)

Murphy, J.B. and Nance, R.D., 2002. Sm-Nd isotopic systematics as tectonic tracers: an example from west Avalonia in the Canadian Appalachians. *Earth-Science Reviews*, 59: 77–100. doi:10.1016/S0012-8252(02)00070-3

Mao, Q.G., Xiao, W.J., Han, C.M., et al., 2010. Discovery of Middle Silurian adaltite granite and its tectonic significance in Liuyuan area, Beishan Moutains, NW China. *Acta Petrologica Sinica*, 26: 584–596 (in Chinese with English abstract)

Mei, W., Lü, X.B., Ai, Z.L., et al., 2014. Geochemistry and zircon U-Pb age of subvolcanic rocks in Dajing deposit, NE China: Geodynamic implications. *Geochemical Journal*, 48: 379–395. doi:10.2343/geochemj.2.0313

Nie, F.J., Jiang S.H., Hu, P. and Zhang, Y. ,2004.Geological features and ore-forming material sources of Hongjianbingshan tungsten deposit in Beishan mountain, Gansu Province. *Mineral Deposits*,23: 11–19 (in Chinese with English abstract)

Peccerillo, R. and Taylor, S.R., 1976. Geochemistry of Eocene calcalkaline volcanic rocks from the Kast amonu area, northern Turkey. *Contributions to Mineralogy and Petrology*,58:63–81. doi: 10.1007/BF00384745

Petford, N., Cmden, A.R., McCaffrey, K.J.W., et al.,2000. Granite magma formation, transport and emplacement in the Earth's cmat. *Nature*,408: 669–673. doi:10.1038/35047000

Pfänder, J.A., Münker, C., Stracke, A. et al., 2007. Nb/Ta and Zr/Hf in ocean island basalts: Implications for crust-mantle differentiation and the fate of niobium. *Earth and Planetary Science Letters*,254:158–172. doi:10.1016/j.epsl.2006.11.027

Ryerson, F.J. and Watson, E.B., 1987. Rutile saturation in magmas: Implications for Ti-Nb-Ta dep letion in island-arc basalts. *Earth and Planetary Science Letters*, 86:225–239. doi:10.1016/0012 -821X(87)90223-8

Rickwood, P.C., 1989. Boundary lines with in petrologic diagram which use oxides of major and minor element. *Lithos*, 22:247–263. doi:10.1016/0024-4937(89)90028-5

Rollinson, H.R., 1993.Using geochemical data: evaluation, presentation, interpretation. London: Longman, 351

Rowley, D.B., Xue, F. and Tucker, R.D., 1997. Ages of ultrahigh pressure metamorphism and protolith orthogneisses from the eastern DabieShan: U/Ph zircon geochronology. *Earth and Planet Science Letters*,151: 191–203. doi:10.1016/S0012-821X(97)81848-1

Sun, S.S. and Mcdonough, W.F., 1989. Chemical and isotopic systematics of oceanic basalts: implications for mantle composition and processes.In : Sanrder, A.D., and Norry, M.J., eds. Magmatism in the ocean basins. *Geological Society of London Special Publication*,42:313–345. doi:10.1144/GSL.SP.19 89.042.01.19

Schmidt, M.W. ,1992. Amphibole composition in tonalite as a function of pressure an experimental calibration of the Al-in-Hornblende barometer. *Contribution to Mineralogy and Petrology*,110: 304–310. doi:10.1007/BF00310745

Sengör, A.M.C., Natal'in, B.A., 1996. Paleotectonics of Asia: Frangments of synthesis. In:Yin, A., Harrison, .M. (Eds.), The Tectonic Evolution of Asia. Cambridge UniversityPress, Cambridge, pp. 480–640

Stevens, G., Villaros, A. and Moyen, J.F., 2007. Selective peritectic garnet entrainment as the origin of geochemical diversity in S-type granites. *Geology*, 35:9–12. doi:10.1080/00206814.2010.543009

Su, B.X., Qin, K.Z., Sakyi, P.A., et al., 2012.Occurrenceof an Alaskan-type complex inthe Middle Tianshan Massif, Central Asian Orogenic Belt: inferences from petrological and mineral ogicalstudies, *International Geology Review*, 54: 249–269. doi:10.1080/00206814.2010.543009

Stepanov, A.S. and Hermann, J., 2013. Fractionation of Nb and Ta by biotite and phengite: Implications for the "missing Nb paradox".*Geology*, 41:303–306. doi:10.1130/G33781.1

Teixeira, R., Neiva, A., Silva, P.B., et al., 2011. Combined U-Pb geochronology and Lu-Hf isotope systematics by LAM-ICP-MS of zircons from granitesand metasedimentary rocks of Carrazeda de Ansiães and Sabugal areas, Portugal, to constrain granite sources. *Lithos*,125: 321–334. doi:10.1016/j.lithos.2011.02.015

Tang, G.J., Wang, Q. and Wyman, D.A., 2013. Petrogenesis of gold-mineralized magmatic rocks of the Taerbieke area, northwestern Tianshan (western China): Constraints from geochronology, geochemist try and Sr-Nd-Pb-Hf isotopic compositions. *Journal of Asian Earth Sciences*,74: 113–128. doi: 10.1016/j.jseaes.2013.03.022

Tang, J.L., 2015. Geological, geochemical characteristics and genesis of Shadong tungsten deposit, Hami，Xinjiang: [Dissertation]. Xinjiang University, 56. (in Chinese)

Visona, D. and Lombardo, B., 2002. Two-mica and tourmaline leucogranites from the Everest-Makalu region (Nepal-Tibet).Himalayan leucogranite genesis by isobaric heating? *Lithos*, 62: 125–150. doi:10.1016/S0024-4937(02)00112-3

Wiedenbeck, M., Alle, P., Corfu, F., et al., 1995. Three natural zirconstandards for U-Th-Pb, Lu-Hf, trace element and REE analyses.*Geostandards Newsletter*,19: 1-23. doi:10.1111/j.1751-908X.1995.tb00147.x

Wickham, S.M., Litvinovsky, B.A., Zanvilevich, A.N. et al., 1996. Geochemical evolution of Phane rozoic magmatism in Transbaikalin, East Asia: a key constraint on the origin of K-rich silicic magmas and the process of cratonization. *Journal of Geophysics Research*, 100: 15641–15654. doi:10.1029/95JB00035

Wu, F.Y., Jahn, B.M., Wilde, S. et al., 2000. Phanerozoic crustal growth: U-Pb and Sr-Nd isotopic evidence from the granites in northeastern China. *Tectonophysics*,328: 89–113. doi:10.1016/S0040-1951(00)00179-7

Wu, F.Y., Jahn, B.M.and Wilder, S.A., 2003.Highly fractionated I-type granites in NE China (I): geochronology and petrogenesis. *Lithos*, 66:241–273. doi:10.1016/S0024-4937(02)00222-0

Whitehouse, M.J., 2003. Rare earth elements in zircon:a review of applications and case studies from the outer Hebridean Lewisian Complex, NW Scotland. In: Vance, D., Muller, W., and Villa, I.M., Geochronology: linking the isotopic record with petrology and textures, *Geological Society, London, SpecialPublications*,220:49–64. doi:10.1144/GSL.SP.2003.220.01.03

Wang, J.H., 2005. Study on geological conditions of ore forming and directions of ore prospecting of tungsten ore deposits in the western Qilian mountains. Master. Sci.Thesis. Chang'an University, 57 (in Chinese)

Wang, T., Hong, D.W., Tong, Y., et al.,2005. Zircon U-Pb SHRIMP age and on origin of post-orogenic Lamazhao granitic pluton from Altai orogen: its implications for vertical continental growth. *Acta Petrologica Sinica*, 21: 640–650 (in Chinese with English abstract)

Wei, S.L., Jia, B.H. and Zeng, Q.W., 2006. Metallogenic mechanism of tungsten deposit in Nanlingarea.

Resource Survey&Environment, 27: 103–109 (in Chinese with English abstract)

Wang, Q., Wyman, D.A. and Zhao, Z.H., 2007. Petrogenesis of Carboniferous adakites and Nb-enriched arc basalts in the Alataw area, northern Tianshan Range (western China): implications for Phanerozoic crustal growth in the Central Asia orogenic belt. *Chemical Geology*,236: 42–64. doi: 10.1016/j.chemgeo.2006.08.013

Wang, T., Li, W.P., Li, J.B., et al.,2008. Increase of juvenal mantle-derived composition from syn-orogenic to post-orogenic granites of east part of the eastern Tianshan (China) and implications for continental vertical growth: Sr and Nd isotopic evidence. *Acta Petrologica Sinica*, 24:762–772 (in Chinese with English abstract)

Wang, Y.J., Yuan, C., Long, X.P., et al., 2011. Geochemistry, zircon U-Ph ages and Hf isotopes of the Paleozoic volcanic rocks in the northwestern Chinese Altai: petrogenesis and tectonic implications. *Journal of Asian Earth Sciences*,42: 969–985. doi:10.1016/j.jseaes.2010.11.005

Wu, Y.S., Xiang, N., Tang, H.S.,et al., 2013. Molybdenite Re-Os isotope age of the Donggebi Mo deposit and the Indosinian metallogenic event in eastern Tianshan. *Acta Petrologica Sinica*, 29: 121–130 (in Chinese with English abstract)

Wang, Y.H., Zhao, C.B., Zhang, F.F., et al.,2015. SIMS zircon U-Pb and molybdenite Re-Os geochronology, Hf isotope, and whole-rock geochemistry of the Wunugetushan porphyry Cu-Mo deposit and granitoids in NE China and their geological significance. *Gondwana Research*, 28: 1228–1245. doi:10.1016/j.gr.2014.10.001

Wang, S., Ye, H.S., Yang, Y.Q. 2016. Zircon U-Pb Chronology, Geochemistry and Hf Isotopic Compositions of the Huoshenmiao Pluton, Western Henan. Earth Science, 41(2): 293–316(in Chinese with English abstract)

Wang, Y.H., Xue, C.J., Liu, J.J., et al. 2016. Geological, geochronological, geochemical, and Sr-Nd-O-Hf isotopic constraints on origins of intrusions associated with the Baishan porphyry Mo deposit in eastern Tianshan, NW China.*Mineralium Deposita*,51(7):953-969. doi:10.1007/s00126-016-0646-z

Wu, Y.S., Zhou, K.F., Li, N., et al.2017.Zircon U-Pb dating and Sr-Nd-Pb-Hf isotopes of the ore-associated porphyry at the giant Donggebi Mo deposit, Eastern Tianshan, NW China. *Ore Geology Reviews*,81:794–807. doi:10.1016/j.oregeorev.2016.02.007

Xiong, X.L., Adam, J. and Green, T.H., 2005. Rutile stability and rutile/melt HFSE partitioning during partial melting of hydrous basalt: implications for TTG genesis *Chemical Geology*, 218: 339–359. doi:10.1016/j.chemgeo.2005.01.014

Xi, B.B., Zhang, D.H. and Zhou, L.M., 2007. Magmatic evolutions of several granite plutons related to Sn (W) miner alizations in the Nanling region, China. *Geological Bulletin of China*, 26:1591–1599 (in Chinese with English abstract)

Xiao, W.J., Windley, B.F., Allen, M.B.,et al., 2013. Paleozoic multiple accretionary and collisional tectonics of the Chinese Tianshan orogenic collage *Gondwana Research*,23: 1316–1341. doi:10.1016/j.gr.2012.01.012

Xiao, W.J. and Santosh, M., 2014. The western Central Asian Orogenic Belt: A window to accret ionaryorogenesis and continental growth. *Gondwana Research*, 25:1429–1444. doi:10.1016/j.gr.2 014.01.008

Xing, X.W.,Wang, Y.J.,and Zhang, Y.Z. 2016. Detrital Zircon U-Pb Geochronology and Lu-Hf Isotopic Compositions of the Wuliangshan Metasediment Rocks in SW Yunnan (China) and Its Provenance Implications. *Journal of Earth Science*, 27(3):412–424. doi:10.1007/s12583-015-0647-3

Xiong, F.H., Ma, C.Q., Jiang, H.A., et al., 2016. Geochronology and Petrogenesis of Triassic High-K Calc-Alkaline Granodiorites in the East Kunlun Orogen, West China: Juvenile Lower Crustal Melting

during Post-Collisional Extension.*Journal of Earth Science*,27(3):474–490. doi:10.1007/s12583-016-0674-6

Yang, W.B., Niu, H.C. and Shan, Q., 2012. Late Paleozoic calc-alkaline to shoshonitic magmatism and its geodynamic implications, Yuxi molegai area, western Tianshan, Xinjiang. *Gondwana Research*, 22: 325–340. doi:10.1016/j.gr.2011.10.008

Zhang, H.F., Gao, S., Zhong, Z.Q., et al., 2002. Geochemical and Sr-Nd-Pb isotopic compositions of Cretaceous granitoids: Constraints on tectonic framework and crustal structure of the Dabie shan ultrahigh-pressure metamorphic belt, China. *Chemical Geology*,186:281–299. doi: 10.1016/S0009-2541(02)00006-2

Zhang Z.Z., 2005a. From the underplating to intraplating: vertical accretion of continental crust and granites in the east section of Mid-Tianshan block. Dr. Sci. Thesis. Nanjing University. 135 (in Chinese)

Zhang, Z.Z., Gu, L.X., Wu, C.Z.,et al., 2005b. Zircon SHRIMP dating for the Weiya pluton, eastern Tianshan: its geological implications. *Acta Geologica Sinica (English edition)*,79: 481–490. doi:10.1111/j.1755-6724.2005.tb00914.x

Zhang, Q., Jin, W.J., Li, C.D., et al., 2010. Revisiting the new classification of granitic rocks based on whole-rock Sr and Yb contents: Index. *Acts Petrologica Sinica*, 26: 985–1015(in Chinese with English abstract)

Zhang, Q., Jin, W.J., Li, C.D., et al., 2011. Granitic rocks and their formation depth in the crust. *Geotectonica et Metallogenia*, 211: 259–269 (in Chinese with English abstract).

Zhai, W., Sun, X.M., and Wu, Y.S., 2012. He-Ar isotope geochemistry of the Yaoling-Meiziwo tungsten deposit, North Guangdong Province: constraints on Yanshanian crust-mantle interaction and metallogenesis in SE China. *Chinese Science Bulletin*, 57: 1150–1159 (in Chinese with English abstract)

Zhu, J., Lü, X.B., Chen, C., Cao, et al., 2013. Geological characteristics, metallogenic time and tectonic setting of the Triassic molybdenum deposits in the east part of the east Tianshan and the Beishan area, NW China. *XinJiang Geology*, 31: 21–28 (in Chinese with English abstract)

Zhou, Z.M., Ma, C.Q.,Xie, C.F., et al.,2016.Genesis of Highly Fractionated I-Type Granites from Fengshun Complex: Implications to Tectonic Evolutions of South China.*Journal of Earth Science*, 27(3):444–460. doi:10.1007/s12583-016-0677-3

Zhao, H.X., Jiang, S.Y., Dai, B.Z. et al., 2016.Geochronology and Hf Isotope Study of Pegmatite in the Xiaoqinling Area of NW China: Implication for Petrogenesis and Regional Metamorphism.*Journal of Earth Science*, 26(3):295–305. doi:10.1007/s12583-015-0537-8

Zhang, W., Zhou, H.W., Zhu, Y.H. 2016. The Evolution of Triassic Granites Associated with Mineralization within East Kunlun Orogenic Belt: Evidence from the Petrology, Geochemistry and Zircon U-Pb Geochronology of the Mohexiala Pluton.*Earth Science*,41(8): 1334–1348(in Chinese with English abstract)